This article has been accepted for publication in a future issue of this journal, but has not been fully edited. Content may change prior to final publication. Citation information: DOI 10.1109/TVT.2016.2580512, IEEE Transactions on Vehicular Technology

Spectral Efficient Quadrature Spatial Modulation Cooperative AF Spectrum-Sharing Systems

Ali Afana, Salama Ikki, Raed Mesleh, and Ibrahem Atawi

***Abstract*—Quadrature spatial modulation (QSM) is a recent multiple-input multiple-output (MIMO) digital transmission paradigm. Combining QSM with cooperative relaying in spectrum-sharing systems improves the overall spectral efficiency and enhances the communication reliability. In this paper, we study the performance of QSM-MIMO amplify-and forward (AF) cooperative relaying spectrum-sharing systems, in which a muti-antenna secondary source communicates with a secondary receiver with a help of a secondary AF relay in the presence of multiple primary receivers. In particular, a closed-form expression for the average pairwise error probability (PEP) of the secondary system is derived and used to obtain a tight upper bound of the average bit error probability (ABEP) over Rayleigh fading channels. In addition, a simple asymptotic, yet accurate, expression is derived and analyzed to show the effect of key parameters. Simulation results are presented to validate numerical analysis. Results reveal that QSM with cooperative relaying improves the spectrum-sharing systems performance.**

***Index Terms*—Amplify-and-forward, Cognitive radio, Quadrature spatial modulation, Spectrum-sharing, MIMO systems.**

I. Introduction

Quadrature spatial modulation (QSM) and spectrum-sharing in cognitive radio (CR) systems are emerging technologies for the next generation (5G) wireless networks [1]. Both techniques promise significant enhancement in the overall system performance without sacrificing power or bandwidth. Hence, studying the performance of the QSM-CR systems is timely and of significant importance for future development. The transmission schemes of QSM [2], spatial modulation (SM) [3], and space-shift-keying (SSK) [4] are proposed as low-complexity and spectral-efficient implementations that avoid conventional multiple-input multiple-output (MIMO) systems' drawbacks including inter-channel interference (ICI) and high receiver complexity [5], [6].

In SM, a single transmit-antenna is activated during each time interval where the index of each transmit antenna conveys a spatial constellation point. The activated antenna transmits a signal constellation symbol from a well-known amplitude/phase constellation diagram. The transmitted symbol carries additional information bits [3]. Meanwhile, QSM is proposed as a new method to further improve the overall spectral efficiency of the conventional SM technique while retaining all inherit advantages of such systems [2]. Specifically, in QSM, the conventional spatial constellation symbols in the SM scheme are further extended to two orthogonal in-phase and quadrature components, i.e., the spatial constellation symbols of SM are expanded to include another dimension. One dimension transmits the real part of the signal constellation symbol and the other dimension transmits the imaginary part of the symbol [2].

Very recently, few works studied QSM in conventional MIMO system over Rayleigh and Nakagami-m fading channels assuming perfect and imperfect channel state information (CSI) [7], [8]. All the aforementioned works studied QSM in traditional point-to-point MIMO systems. Our work in [9] extended the QSM technique to amplify-and-forward (AF) relaying systems, where upper-bound and asymptotic average error probabilities were obtained. Recently, adaptive SM for spectrum-sharing systems was proposed in [10] to enhance the spectral efficiency. In [11], authors studied the error performance of SM-MIMO spectrum-sharing systems with channel estimation errors. Authors in [12] studied QSM-MIMO in CR networks where imperfect CSI was assumed. To the best of our knowledge, there exists no work in the literature studying QSM cooperative spectrum-sharing systems.

In this work, the average bit error probability (ABEP) for QSM-AF cooperative spectrum-sharing systems is analyzed. Specifically, a multi-antenna secondary source communicates with a secondary destination via a secondary AF relay in the presence of multiple primary receivers, in both, broadcasting and relaying phases. A mean-value power allocation method is used to allocate the secondary transmitters' (source and relay) transmit powers, where a limited CSI feedback from the primary receivers is assumed to be available. To investigate the secondary system performance, a closed-form expression for the average pairwise error probability (PEP) is derived employing the optimal maximum likelihood (ML) detector at the secondary receivers. Based on the derived PEP expression, a tight upper bound expression for the ABEP is obtained using the union bound formula. Moreover, an asymptotic analysis is performed to get insights on the key parameters, including the diversity and the number of transmit antennas. The results demonstrate the effectiveness of combining QSM and cooperative relaying in improving the overall system performance.

The remainder of this paper is organized as follow: Section II describes system and channel models. Performance analysis is presented in Section III. Numerical results are presented in

Ali Afana and Salama Ikki are with Department of Electrical Engineering, Faculty of Engineering, Lakehead University, Ontario, Canada, E-mails: {aafana, sikki}@lakeheadu.ca.

Raed Mesleh is with the Electrical and Communications Engineering Department, School of Electrical Engineering and Information Technology, German Jordanian University, Amman 11180, Jordan (e-mail: raed.mesleh@gju.edu.jo).

Ibrahem Atawi is with University of Tabuk, Electrical Engineering Department, Faculty of Engineering, P.O.Box:741, 71491 Tabuk, Saudi Arabia, e-mail: {ieatawi@ut.edu.sa}

This article has been accepted for publication in a future issue of this journal, but has not been fully edited. Content may change prior to final publication. Citation information: DOI 10.1109/TVT.2016.2580512, IEEE Transactions on Vehicular Technology

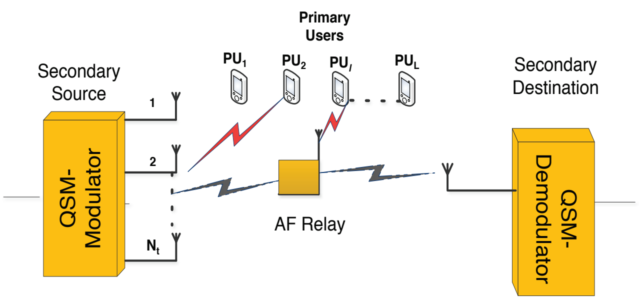

Fig. 1: System model of a QSM-AF CR system.

Section IV. Finally, Section V concludes the paper.

Notations: $\Pr(\cdot)$ denotes the probability of an event. E[X] and VAR[X] denote the mean and variance of a random variable (r.v.) X, respectively. $X \sim CN(0, \sigma_X^2)$ represents a complex-valued Gaussian r.v. with a zero mean and variance σ_X^2. $\mathrm{Re}\{X\}$ denotes the real part of the complex value r.v. X. PDF refers to the probability density function and CDF refers to cumulative distribution function.

II. System Model

A. Channel Model

We consider a QSM cooperative spectrum-sharing AF relaying system model comprising a secondary source S with N_t transmit antennas, a single antenna AF relay R, a single antenna secondary destination D and L multiple primary receivers (PU-Rx) as depicted in Fig. 1. The cooperative system is operating over Rayleigh fading channels. We assume that $b = \log_2(MN_t^2)$ incoming bit stream enters the source at each transmission instant. The incoming data bits are processed and partitioned into three groups. S determines the index of the active transmit antennas by using two groups of $\log_2(N_t)$ bits of b, then maps the remaining $\log_2(M)$ bits onto the corresponding M-ary quadrature amplitude modulation (M-QAM)/ phase shift keying (M-PSK) or other complex signal constellation diagrams. The signal constellation symbol, x, is further decomposed to its real, $x_\Re$, and imaginary, $x_\Im$, parts. The real part is transmitted from one transmit antenna among the existing N_t transmit antennas, where the active antenna index is determined by the first $\log_2(N_t)$ bits. Similarly, the imaginary part is transmitted by another or the same transmit antenna depending on the other $\log_2(N_t)$ bits. However, the transmitted real and imaginary parts are orthogonal representing the in-phase and the quadrature components of the carrier signal.

An example for QSM bits mapping and transmission is given in what follows assuming (4×1)-MISO system and 4-QAM modulation. The number of data bits that can be transmitted at one particular time instant is $b = \log_2(N_t^2 M) = 6$ bits. Assume that the following incoming data bits, $b = \underbrace{\left[\begin{array}{cccccc} 0 & 1 & 1 & 0 & 1 & 1 \end{array}\right]}_{\log_2(M)+\log_2(N_t^2)}$ are to be transmitted. The first $\log_2(M)$ bits $\left[\begin{array}{cc} 0 & 1 \end{array}\right]$, modulate a 4-QAM symbol, $x = -1 + j$. This symbol is divided further into real and imaginary parts, $x_\Re = -1$ and $x_\Im = 1$. The second $\log_2(N_t)$ bits $\left[\begin{array}{cc} 1 & 0 \end{array}\right]$, modulate the active antenna index, $\ell_\Re = 3$ to transmit $x_\Re = -1$ resulting in the transmitted vector $\mathbf{s}_\Re = \left[\begin{array}{cccc} 0 & 0 & -1 & 0 \end{array}\right]^T$. The last $\log_2(N_t)$ bits, $\left[\begin{array}{cc} 1 & 1 \end{array}\right]$, modulate the active antenna index, $\ell_\Im = 4$, used to transmit $x_\Im = 1$, resulting in the vector $\mathbf{s}_\Im = \left[\begin{array}{cccc} 0 & 0 & 0 & 1 \end{array}\right]^T$. The transmitted vector is then obtained by adding the real and imaginary vectors, $\mathbf{s} = \mathbf{s}_\Re + j\mathbf{s}_\Im = \left[\begin{array}{cccc} 0 & 0 & -1 & +j \end{array}\right]^T$.

B. Secondary Power Allocation Method

In the underlay CR approach, S can use the PUs' spectrum as long as the interference it generates to the most affected PU-Rx remains below a predefined threshold I_{p_1}. In general, the PU-Rx is assumed to know the interference channel gain (or its estimate) [13]. Therefore, it can calculate the mean value (MV) of this gain. Then, the estimated arithmetic MV (a constant) is fed back to the S. Consequently, the adoption of the MV-power allocation can considerably reduce the feedback burden [13] when compared to the scheme which requires instantaneous channel state information (CSI) feedback on every symbol unit or block of symbols. Therefore, the source's transmission power P_S is constrained as $P_S = \min\left(\frac{I_{p_1}}{\max\limits_{l=1,2,\ldots,L} \mathrm{E}(|\hat{f}_{t,l}|^2)}, P_m\right)$, where $\hat{f}_{t,l}$ is the estimated channel coefficient between the t^{th} transmit antenna and the l^{th} PU-Rx with $\mathrm{E}(|\hat{f}_{t,l}|^2) = \lambda_{t,l}$ and P_m is the maximum available power at S. Similarly, the relay's transmission power P_r is constrained as $P_r = \min\left(\frac{I_{p_2}}{\max\limits_{l=1,2,\ldots,L} \mathrm{E}(|\hat{f}_{r,l}|^2)}, P_{m_o}\right)$, where $\hat{f}_{r,l}$ is the estimated channel coefficient between the relay and the l^{th} PU-Rx with $\mathrm{E}(|\hat{f}_{r,l}|^2) = \lambda_{r,l}$ and P_{m_o} is the maximum available power at R.

The transmission protocol occurs over two time slots in two phases as shown in Fig. 1. In the first phase, based on the interference CSI between the activated antenna at S and the most affected PU-Rx, i.e. (the strongest interference channel), S adjusts its transmit power under a predefined threshold I_{p_1} and broadcasts its message to the relay. Any data transmitted from S resulting in an interference level higher than I_{p_1}, which is the maximum tolerable interference power level at PU-Rx, is not allowed. Herewith, the vector, $\mathbf{s}$, is transmitted to the relay , over an $N_t \times 1$ Rayleigh fading wireless channel, denoted as, $\mathbf{h}$. Hence, in the first phase, the received signal at R can be written as

$$y_{s,r} = \sqrt{\frac{P_S}{2}} h_{\ell_\Re} x_\Re + j\sqrt{\frac{P_S}{2}} h_{\ell_\Im} x_\Im + \eta_r, \qquad (1)$$
$$\ell_\Re, \ell_\Im = 1, 2, \cdots, N_t;$$

where $x_\Re$ and $x_\Im$ are symbols in the PAM signal-constellation diagram and $h_{\ell_\Re}$ and $h_{\ell_\Im}$ are the channel coefficients between the activated antennas and the relay's antenna, which are assumed to be complex Gaussian random variables with zero mean and variances σ_h^2, and $\eta_r \sim CN(0, N_0)$ is the complex Gaussian noise with zero mean and variance N_0 .

Similarly, in the second phase, based on the interference CSI between the relay and the most affected PU-Rx, the AF relay adjusts its transmit power under a predefined threshold I_{p_2} and

This article has been accepted for publication in a future issue of this journal, but has not been fully edited. Content may change prior to final publication. Citation information: DOI 10.1109/TVT.2016.2580512, IEEE Transactions on Vehicular Technology

forwards the amplified signal to the destination. In particular, the relayed signal (x_R) is an amplified version of the input signal at the relay node, i.e., $x_R = A \times y_{s,r}$, where A is the amplification factor. Using this technique, the amplification process is performed in the analogue domain and consists of a simple normalization of the total received power without further processing. Hence, the received signal at D from R in the second phase can be written as

$$\begin{aligned} y_{r,d} &= Ag y_{s,r} + n_{r,d} \\ &= \underbrace{Ag\sqrt{\frac{P_S}{2}} h_{\ell_\Re} x_\Re + jAg\sqrt{\frac{P_S}{2}} h_{\ell_\Im} x_\Im}_{\text{Signal Part}} + \underbrace{Ag\eta_r + n_{r,d}}_{\text{Noise Part}}, \end{aligned} \tag{2}$$

where $n_{r,d}$ denotes the AWGN at the secondary receiver. Then, by dividing all terms by $\sqrt{A^2|g|^2+1}$, it gives

$$\begin{aligned} y_{r,d} = &\frac{Ag}{\sqrt{A^2|g|^2+1}}\sqrt{\frac{P_S}{2}} h_{\ell_\Re} x_\Re + j\frac{Ag}{\sqrt{A^2|g|^2+1}} \\ &\times \sqrt{\frac{P_S}{2}} h_{\ell_\Im} x_\Im + \hat{n}, \end{aligned} \tag{3}$$

where g is the coefficient channel fading between R and D, $A = \sqrt{\frac{1}{P_S\sigma_h^2/2+N_0}}$, and $\hat{n}$ is the Gaussian noise with variance N_0.

C. ML Detection

Since the channel inputs are assumed equally likely, the optimal detector, based on the ML principle, is given as

$$\begin{aligned} &[\ell_\Re, \ell_\Im, x_\Re, x_\Im] = \\ &\arg\min_{\ell_\Re,\ell_\Im,x_\Re,x_\Im} \left\| y_{r,d} - \frac{Ag}{\sqrt{A^2|g|^2+1}}\sqrt{\frac{P_S}{2}}\left[h_{\ell_\Re}x_\Re + jh_{\ell_\Im}x_\Im\right]\right\|^2 \\ &= \arg\min_{\ell_\Re,\ell_\Im,x_\Re,x_\Im} ||\mathcal{C}||^2 - 2\Re\left\{y_{r,d}^H \mathcal{C}\right\}, \end{aligned} \tag{4}$$

where $\mathcal{C} = \frac{Ag}{\sqrt{A^2|g|^2+1}}\sqrt{\frac{P_S}{2}}\left[h_{\ell_\Re}x_\Re + jh_{\ell_\Im}x_\Im\right]$. It can be seen that optimal detection requires a joint detection of the antenna indices and data symbols.

III. Performance Analysis

In this section, the ABEP performance is investigated for any M-ary coherent modulation scheme. First, a closed-form expression for the average PEP is derived, from which, we derive a tight upper bound ABEP expression. Second, we analyze the asymptotic performance of the system.

A. Signal-to-noise ratio (SNR) statistics

Assuming $\mathcal{C}$ is transmitted, the probability of deciding in favor of $\hat{\mathcal{C}} = \frac{Ag}{\sqrt{A^2|g|^2+1}}\sqrt{\frac{P_S}{2}}\left[\hat{h}_{\ell_\Re}\hat{x}_\Re + j\hat{h}_{\ell_\Im}\hat{x}_\Im\right]$, i.e. (error event) is given as

$$\Pr\left(\mathcal{C} \to \hat{\mathcal{C}}|\mathbf{h}\right) = Q\left(\sqrt{\gamma}\right) \tag{5}$$

where $\hat{h}_{\ell_\Re}$ and $\hat{h}_{\ell_\Im}$ are the error decisions of $h_{\ell_\Re}$ and $h_{\ell_\Im}$, respectively. We define γ as

$$\gamma \equiv \frac{1}{2N_0} \parallel \mathcal{C} - \hat{\mathcal{C}} \parallel^2 = \frac{A^2|g|^2}{A^2|g|^2+1}\frac{P_S}{4N_0}|\kappa + j\mu|^2, \tag{6}$$

where

$$\kappa = \left(h^R_{\ell_\Re}x_\Re - h^I_{\ell_\Im}x_\Im - \hat{h}^R_{\ell_\Re}\hat{x}_\Re + \hat{h}^I_{\ell_\Im}\hat{x}_\Im\right). \tag{7}$$

$$\mu = \left(h^I_{\ell_\Re}x_\Re + h^R_{\ell_\Im}x_\Im - \hat{h}^I_{\ell_\Re}\hat{x}_\Re - \hat{h}^R_{\ell_\Im}\hat{x}_\Im\right). \tag{8}$$

where the notations $(\cdot)^R$ and $(\cdot)^I$ refer to the real part and the imaginary part of the channel coefficient, respectively. Since the symbols $x_\Re$ and $x_\Im$ are drawn from a real constellation, i.e., pulse amplitude modulation (PAM), κ and μ are independent. After a few algebraic manipulations,

$$\Pr\left(\mathcal{C} \to \hat{\mathcal{C}}|\mathbf{h}\right) = Q\left(\sqrt{\frac{\Lambda\Theta}{\Lambda+\Psi}}\right), \tag{9}$$

where $\gamma = \frac{\Lambda\Theta}{\Lambda+\Psi}$, $\Lambda = \frac{P_R|g|^2}{N_0}$, and $\Psi = \frac{P_R}{N_0 A^2}$, and $\Theta = \frac{P_S}{4N_0}|\kappa + j\mu|^2$. Note that Θ is an exponential random variable with the following mean

$$\bar{\Theta} = \begin{cases} \frac{\min\left(\frac{I_p}{\max_{l=1,2,\ldots,L} \mathrm{E}(|\hat{f}_{t,l}|^2)}, P_m\right)}{4N_0}\sigma_h^2\Xi_1 & \text{if } h_{\ell_\Re} \neq \hat{h}_{\ell_\Re}, h_{\ell_\Im} \neq \hat{h}_{\ell_\Im}, \\ \frac{\min\left(\frac{I_p}{\max_{l=1,2,\ldots,L} \mathrm{E}(|\hat{f}_{t,l}|^2)}, P_m\right)}{4N_0}\sigma_h^2\Xi_2 & \text{if } h_{\ell_\Re} = \hat{h}_{\ell_\Re}, h_{\ell_\Im} \neq \hat{h}_{\ell_\Im}, \\ \frac{\min\left(\frac{I_p}{\max_{l=1,2,\ldots,L} \mathrm{E}(|\hat{f}_{t,l}|^2)}, P_m\right)}{4N_0}\sigma_h^2\Xi_3 & \text{if } h_{\ell_\Re} \neq \hat{h}_{\ell_\Re}, h_{\ell_\Im} = \hat{h}_{\ell_\Im}, \\ \frac{\min\left(\frac{I_p}{\max_{l=1,2,\ldots,L} \mathrm{E}(|\hat{f}_{t,l}|^2)}, P_m\right)}{4N_0}\sigma_h^2\Xi_4 & \text{if } h_{\ell_\Re} = \hat{h}_{\ell_\Re}, h_{\ell_\Im} = \hat{h}_{\ell_\Im}, \end{cases} \tag{10}$$

where $\Xi_1 = \left(|x_\Re|^2 + |\hat{x}_\Re|^2 + |x_\Im|^2 + |\hat{x}_\Im|^2\right)$, $\Xi_2 = \left(|x_\Re - \hat{x}_\Re|^2 + |x_\Im|^2 + |\hat{x}_\Im|^2\right)$, $\Xi_3 = \left(|x_\Re|^2 + |\hat{x}_\Re|^2 + |x_\Im - \hat{x}_\Im|^2\right)$, and $\Xi_4 = \left(|x_\Re - \hat{x}_\Re|^2 + |x_\Im - \hat{x}_\Im|^2\right)$.

Furthermore, if we assume quadrature space shift keying (QSSK), which is defined as a special case of the QSM (the spatial constellation dimensions are used only to convey the transmitted data without using any additional M-ary modulation schemes [4]), i.e., $|x_\Re|^2 = |x_\Im|^2 = 1$, $\bar{\Theta}$ can be simplified to

$$\bar{\Theta} = \begin{cases} \frac{\min\left(\frac{I_p}{\max_{l=1,2,\ldots,L} \mathrm{E}(|\hat{f}_{t,l}|^2)}, P_m\right)}{N_0}\sigma_h^2 \\ \quad \text{if } h_{\ell_\Re} \neq \hat{h}_{\ell_\Re}, h_{\ell_\Im} \neq \hat{h}_a, \\ \frac{\min\left(\frac{I_p}{\max_{l=1,2,\ldots,L} \mathrm{E}(|\hat{f}_{t,l}|^2)}, P_m\right)}{2N_0}\sigma_h^2 \\ \text{if } h_{\ell_\Re} = \hat{h}_{\ell_\Re}, h_{\ell_\Im} \neq \hat{h}_{\ell_\Im}, \text{ or } h_{\ell_\Re} \neq \hat{h}_{\ell_\Re}, h_{\ell_\Im} = \hat{h}_{\ell_\Im} \end{cases} \tag{11}$$

To find the average error probability, the CDF of γ should be obtained. This can be done as follows: The PDF of Λ is $f_\Lambda(x) = \frac{1}{\bar{\Lambda}}\exp\left(-\frac{x}{\bar{\Lambda}}\right)$, where $\bar{\Lambda} = \sigma_g^2 P_R/N_0$, and the PDF of Θ is $f_\Theta(x) = \frac{1}{\bar{\Theta}}\exp(-x/\bar{\Theta})$. Therefor, the CDF of γ is

This article has been accepted for publication in a future issue of this journal, but has not been fully edited. Content may change prior to final publication. Citation information: DOI 10.1109/TVT.2016.2580512, IEEE Transactions on Vehicular Technology

derived as [9]

$$F_\gamma(x) \quad = 1 - 2\sqrt{\frac{\Psi x}{\bar{\Theta}\bar{\Lambda}}} \exp\left(-\frac{x}{\bar{\Theta}}\right) K_1\left(2\sqrt{\frac{\Psi x}{\bar{\Theta}\bar{\Lambda}}}\right), \quad (12)$$

where $K_v(.)$ is the v^{th}-order modified Bessel function of the second kind.

B. Exact Average PEP

The alternative expression of the average pairwise error probability can be written as

$$\text{PEP} = \frac{a}{2}\sqrt{\frac{b}{2\pi}} \int_0^\infty \frac{1}{\sqrt{x}} \exp\left(-\frac{bx}{2}\right) F_\gamma(x) dx, \quad (13)$$

where (a, b) values depend on the M-ary modulation scheme adopted. Substituting (12) into (13) and solve the integral with the help of [14, 6.614.5, pp.698], it yields

$$\text{PEP} = \frac{1}{2} - \frac{1}{2}\frac{\Psi}{\bar{\Lambda}\left(2+\bar{\Theta}\right)}\sqrt{\frac{\bar{\Theta}}{2+\bar{\Theta}}} \exp\left(\frac{\Psi}{\bar{\Lambda}\left(2+\bar{\Theta}\right)}\right) \times \left[K_1\left(\frac{\Psi}{\bar{\Lambda}\left(2+\bar{\Theta}\right)}\right) - K_0\left(\frac{\Psi}{\bar{\Lambda}\left(2+\bar{\Theta}\right)}\right)\right]. \quad (14)$$

This closed-form expression of PEP in (14) is used in evaluating an upper bound expression for the ABEP performance for the considered system model.

C. ABEP Performance

After the evaluation of the average PEP, the ABEP of the proposed scheme can be upper bounded by the following asymptotically tight union bound [15]

$$\text{ABEP} = \frac{1}{2^b}\sum_{n=1}^{2^b}\sum_{m=1}^{2^b}\frac{1}{b}\Pr(\mathcal{C}_n \to \mathcal{C}_m) e_{n,m}, \quad (15)$$

where $\{\mathcal{C}_n\}_{n=1}^{2^b}$ is the set of all possible QSM symbols, $b = \log_2(MN_t^2)$ is the number of information bits per QSM symbol, and $e_{n,m}$ is the number of bit errors associated with the corresponding PEP event. Note that M represents the size of the constellation diagram.

D. Asymptotic Analysis

Although the expressions for the average error probability in (14) enables numerical evaluation of the system performance and may not be computationally intensive, it does not offer insight into the effect of the system parameters. We now aim at expressing $F_\gamma(x)$ and the average PEP in simpler forms.

According to [16], the asymptotic error probability can be derived based on the behavior of the CDF of γ around the origin. By using Taylor's series, $F_\gamma(x)$ can be rewritten as

$$F_\gamma(x) \approx \left(\frac{1}{\bar{\Theta}} + \frac{\Psi}{\bar{\Theta}\bar{\Lambda}}\left(\psi(1) - \log\left(\frac{\Psi}{\bar{\Theta}\bar{\Lambda}}\right)\right)\right) x + \text{H.O.T}, \quad (16)$$

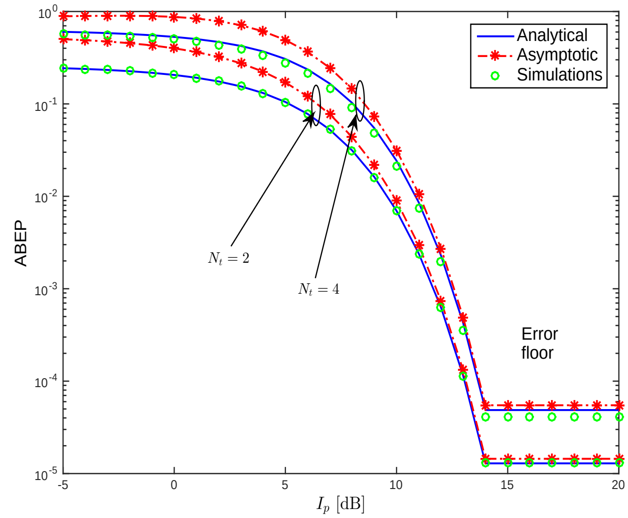

Fig. 2: Analytical, simulation and asymptotic ABEP vs. I_p (dB) with $N_t = 2, 4$, and 4-QAM scheme.

where $\psi(.)$ is the Digamma function, note that $\psi(1) = -0.57721$ [14] and H.O.T refers to higher order terms. Substituting (16) into (13) and solve the integration we have

$$\text{PEP} \approx \frac{1}{2}\left(\frac{1}{\bar{\Theta}} + \frac{\Psi}{\bar{\Theta}\bar{\Lambda}}\left(\psi(1) - \log\left(\frac{\Psi}{\bar{\Theta}\bar{\Lambda}}\right)\right)\right). \quad (17)$$

It can observed from (17) that all the parameters are constants, hence, the system performance saturates to a constant value due to interference and transmit power constraints. However, in the low to medium region of SNR values, there is a diversity, i.e. the error curve goes to zero asymptotically. It is worth to mention that, in next section, it is shown that this asymptotic expression in (17) is tight for pragmatic SNR values.

IV. Numerical analysis and Discussion

In this section, the performance of QSM AF cooperative relaying system is evaluated via analytical results and validated through simulations. Unless otherwise stated, we assume $L = 2$, $\sigma_h^2 = 1, N_0 = 1, \lambda_{t,l} = \lambda_{r,l}, M = 4$, $P_m = P_{m_o} = 20$ dB, and $I_{p_1} = I_{p_2} = I_p$.

In Fig. 2, the ABEP versus I_p is evaluated and simulated for $N_t = 2, 4$. Due to the effect of combined QSM and cooperative relaying, it can be observed that the ABEP performance improves when I_p increases, i.e., the interference constraint becomes less strict. Note that the improvement gain is attained at almost no cost. The receiver complexity of QSM depends on the considered spectral efficiency as reported in [2]. In the high region, the asymptotic ABEP performance becomes in excellent agreement with exact one and saturates to a constant value (error floor). This saturation occurs due to the maximum power limitation constraint.

In Fig. 3, the ABEP is simulated and evaluated versus $\lambda_{t,l}$ for different values of $I_p = 2, 5, 7$. When $\lambda_{t,l}$ increases, the performance improves. This is because the most affected interference channel becomes weaker. In addition, increasing the value of I_p means that the secondary source is allowed

This article has been accepted for publication in a future issue of this journal, but has not been fully edited. Content may change prior to final publication. Citation information: DOI 10.1109/TVT.2016.2580512, IEEE Transactions on Vehicular Technology

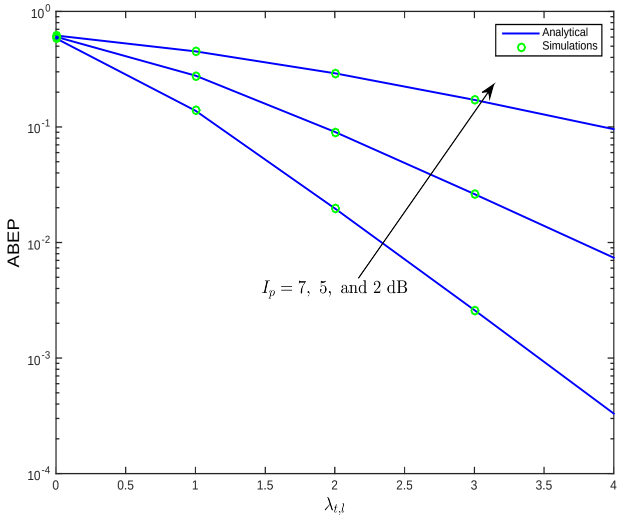

Fig. 3: ABEP vs. $\lambda_{t,l}$ with $N_t = 2, L = 2$, and 4-QAM scheme for different interference thresholds $I_p = 2, 5, 7$.

to transmit with higher transmit power as if it is a non-cognitive scheme (loose constraint). It is noted, in all figures, that there is an excellent agreement between the analytical and simulation results, which corroborate the exactness of the conducted analysis.

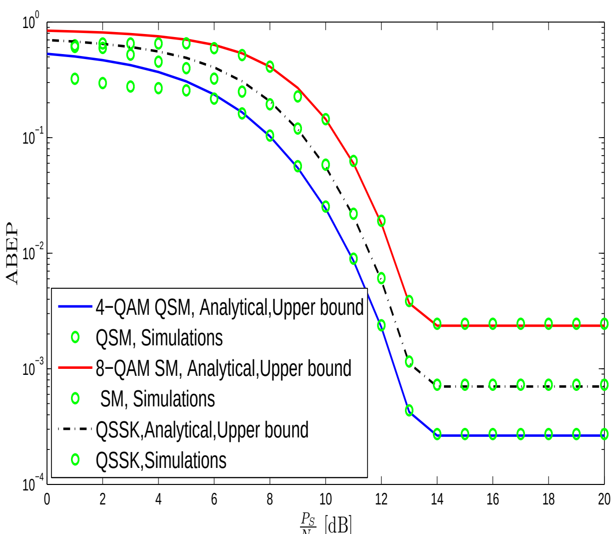

Fig. 4: ABEP vs. $\frac{P_S}{N_0}$ with $I_p = 5$ dB, $L = 2$, for 4-QAM QSM, 8-QAM SM, and QSSK schemes.

In Fig. 4, the ABEP performance of QSM-AF scheme is evaluated and simulated versus P_S/N_0 dB for different modulation schemes, including 4-QAM QSM and 8-QAM SM at same $I_p = 5$ dB and $N_t = 2$. For fair comparison, we include the performance of QSSK-AF scheme with $N_t = 4$ to have similar spectral efficiency with 4-QAM QSM-AF scheme. It is observed that there is a gain of 2 dB for 4-QAM QSM scheme over the QSSK scheme and about 3 dB gain over SM scheme for the same spectral efficiency 4 bits/sec/Hz at the cost of the system (receiver and transmitter) complexity.

Please note that the tightness of the upper bound in (15) strongly depends on the system configurations. In Fig. 2, the bound is shown to be tight for $N_t = 2$ and a bit loose for $N_t = 4$. Also, in Fig. 4, considering higher modulation order such as 8-QAM, the bound is shown to be loose at low SNR values.

V. Conclusions

We analyzed the performance of QSM-AF cooperative spectrum-sharing systems employing ML detector at the secondary destination. A tight upper bound expression for the ABEP was derived using the closed-form expression for the average PEP. In addition, the asymptotic performance analysis was performed; where a simple approximate error expression was derived at pragmatic SNR values. The combined QSM cooperative system enhances the secondary system performance while achieving higher spectral efficiency and maintaining most of SM-AF inherent advantages without requiring any additional receiver complexity.

References

[1] W. Cheng-Xiang *et al.*, "Cellular architecture and key technologies for 5G wireless communication networks," *IEEE Commun. Mag.*, vol. 52, no. 2, pp. 122–130, Feb. 2014.

[2] R. Mesleh, S. Ikki, and H. Aggoune, "Quadrature spatial modulation," *IEEE Trans. Veh. Tech.,* vol. 64, no. 6, pp. 2738–2742, Jun. 2015.

[3] R. Mesleh, H. Haas, S. Sinanović, C. W. Ahn, and S. Yun, "Spatial modulation," *IEEE Trans. Veh. Tech.,* vol. 57, no. 4, pp. 2228–2241, Jul. 2008.

[4] R. Mesleh, S. Ikki, E. Aggoune, and A. Mansour, "Performance analysis of space shift keying (SSK) modulation with multiple cooperative relays", *EURASIP Journal on Advances in Signal Processing,* vol. 1, pp.1–10, 2012.

[5] P. Yang, M. Di Renzo, Y. Xiao, S. Li, and L. Hanzo, "Design guidelines for spatial modulation," *IEEE Commun. Surveys Tut.,* vol. 17, no. 1, pp. 6–26, Mar. 2015.

[6] E. Basar, U. Aygolu, E. Panayirci, and H. V. Poor, "Performance of spatial modulation in the presence of channel estimation errors," *IEEE Commun. Lett.,* vol. 16, no. 2, pp. 176–179, Feb. 2012.

[7] R. Mesleh and S. Ikki, "A high spectral efficiency spatial modulation technique," in *Proc. IEEE Vehicular Technology Conference (VTC Fall)*, pp.1–5, 14-17 Sept. 2014.

[8] A. Younis, R. Mesleh, and H. Haas, "Quadrature spatial modulation performance over Nakagami-m fading channels," *IEEE Trans. Veh. Tech.,* 2015.

[9] A. Afana, R. Mesleh, S. Ikki and I. E. Atawi, "Performance of quadrature spatial modulation in amplify-and-forward cooperative relaying," *IEEE Commun. Lett.,* vol. 20, no. 2, pp. 240–243, Feb. 2016.

[10] Z. Bouida, A. Ghrayeb, and K. Qaraqe, "Adaptive spatial modulation for spectrum sharing systems with limited feedback," *IEEE Trans. Commun.,* vol. 63, no. 6, pp. 2001–2014, Jun. 2015.

[11] A. Afana, T. Ngatched, and O. Dobre, "Spatial modulation in MIMO limited-feedback spectrum-sharing systems with mutual interference and channel estimation errors," *IEEE Commun. Lett.,* vol. 19, no. 10, pp. 1754–1757, Oct. 2015.

[12] A. Afana, I. Atawi, S. Ikki, and R. Mesleh, "Energy efficient quadrature spatial modulation MIMO cognitive radio networks with imperfect channel estimation", in *IEEE ICUWB 2015 workshops*, Oct. 2015.

[13] K. Tourki, F. A. Khan, K. A. Qaraqe, Y. Hong-Chuan, and M.-S. Alouini, "Exact performance analysis of MIMO cognitive radio systems using transmit antenna selection," *IEEE J. Sel. Areas in Commun.,* vol. 32, no. 3, pp. 425–438, Mar. 2014.

[14] I. S. Gradshteyn and I. M. Ryzhik, *Table of Integrals, Series and Products*, 7th ed. Elsevier, 2007.

[15] J. Proakis, *Digital Communications,* 4th ed. McGraw-Hill, 2000.

[16] S. S. Ikki, "Performance analysis of cooperative diversity networks with imperfect channel estimation over Rician fading channels", *IET Signal Processing*, vol. 6, no. 6, pp. 577–583, 2012.